PROCEEDINGS OF SPIE

SPIEDigitalLibrary.org/conference-proceedings-of-spie

VINYL: The VIrtual Neutron and x-raY Laboratory and its applications

E, J. C., Hafner, A., Kluyver, T., Bertelsen, M., Upadhyay Kahaly, M., et al.

J. C. E, A. Hafner, T. Kluyver, M. Bertelsen, M. Upadhyay Kahaly, Z. Lecz, S. Nourbakhsh, A. P. Mancuso, C. Fortmann-Grote, "VINYL: The VIrtual Neutron and x-raY Laboratory and its applications," Proc. SPIE 11493, Advances in Computational Methods for X-Ray Optics V, 114930Z (21 August 2020); doi: 10.1117/12.2570378

SPIE.

Event: SPIE Optical Engineering + Applications, 2020, Online Only

VINYL: The VIrtual Neutron and x-raY Laboratory and its applications

J. C. E[a], A. Hafner[b], T. Kluyver[a], M. Bertelsen[c], M. Upadhyay Kahaly[d], Z. Lecz[d], S. Nourbakhsh[e], A. P. Mancuso[a], and C. Fortmann-Grote[af]

[a]European XFEL GmbH, Holzkoppel 4, 22869 Schenefeld, Germany
[b]CERIC-ERIC, S.S. 14 - km 163,5 in AREA Science Park, Trieste, Italy
[c]European Spallation Source ERIC,P.O. Box 176, SE-22100 Lund, Sweden
[d]ELI-HU, Wolfgang Sandner utca 3., H-6728 Szeged, Hungary
[e]Institut Laue-Langevin, 71 avenue des Martyrs, CS 20156, 38042 Grenoble Cedex 9, France
[f]Max Planck Institute for Evolutionary Biology, August-Thienemann-Straße 2, 24306 Plön, Germany

ABSTRACT

Experiments conducted in large scientific research infrastructures, such as synchrotrons, free electron lasers and neutron sources become increasingly complex. Such experiments, often investigating complex physical systems, are usually performed under strict time limitations and may depend critically on experimental parameters. To prepare and analyze these complex experiments, a virtual laboratory which provides start-to-end simulation tools can help experimenters predict experimental results under real or close to real instrument conditions. As a part of the PaNOSC (Photon and Neutron Open Science Cloud) project, the VIrtual Neutron and x-raY Laboratory (VINYL) is designed to be a cloud service framework to implement start-to-end simulations for those scientific facilities. In this paper, we present an introduction of the virtual laboratory framework and discuss its applications to the design and optimization of experiment setups as well as the estimation of experimental artifacts in an X-ray experiment.

Keywords: start to end simulation, X-ray, neutron, diffraction, python, PaNOSC, EOSC

1. INTRODUCTION

In the past a few decades, there have been many efforts in technologically improving X-ray and neutron research infrastructures (RIs). Along with the increasing brilliance and repetition rate of the scientific infrastructures, the experiments conducted there become increasingly complex. Being limited by the number of experiment end-stations in these RIs, obtaining experimental time (so-called beamtime) becomes difficult with demand far exceeding supply. Even if beamtime is obtained, such experiments are always under strict time limitations, and are thus challenging to prepare. Additionally, the properties of various samples and methodologies implemented require different machine parameters, such as X-ray/neutron energy, pulse duration and diffraction geometry, which makes such experiments relatively complicated. To prepare for such a experiment, it is desirable to possess a thorough simulation, accounting from the source of the beam to the signal captured by the detector, to generate supporting material for beamtime proposals including estimating the optimal parameters for each step of the experiment, as well as helping in the interpretation of experimental results.

The PaNOSC project,[1] Photon and Neutron Open Science Cloud, aims to contribute to the construction and development of the European Open Science Cloud (EOSC), an ecosystem allowing universal and cross-disciplinary open access to data through a single access point, for researchers in all scientific fields. The participants include ESRF, CERIC-ERIC, ELI Delivery Consortium, the European Spallation Source, European XFEL and the Institut Laue-Langevin – ILL, and the e-infrastructures EGI and GEANT.

Further author information: (Send correspondence to J. C. E)
J. C. E: E-mail:juncheng.e@xfel.eu

Advances in Computational Methods for X-Ray Optics V, edited by Oleg Chubar, Kawal Sawhney,
Proc. of SPIE Vol. 11493, 114930Z · © The Authors. Published under a Creative Commons
Attribution CC-BY 3.0 License · doi: 10.1117/12.2570378

As workpackage 5 of the PaNOSC project, the VIrtual Neutron and x-raY Laboratory (VINYL) is designed to be a virtual facility providing a simulation capability from the source to the detector representing all major components of real photon and neutron RIs. By harmonizing existing "state-of-the-art" simulation tools, VINYL should ultimately provide the functionality to simulate whole experiments with various parameters at each part of the experimental instrument. The simulations can help estimate the most optimal experimental environment based on the final simulated data quality for a particular experiment. Ultimately, the simulation results are expected to be stored and shared in a open science database to benefit the broader scientific community.

In this paper, we will first describe the architecture of the VINYL simulation platform, and then we will introduce the simulation examples of the X-ray Gaussian source simulation, serial crystallography simulation, and polychromatic diffraction simulation, showing the potential of the VINYL project.

2. THE ARCHITECTURE OF VINYL

The elements of VINYL are schematically shown in the block diagram Fig. 1. On the top is the simulation platform providing the user interface connecting users' commands and the computing resources. The user can choose to either use a Jupyter Notebook[2] through a JupyterHub service or use a remote desktop service. The simulation platform will provide a harmonized Application Program Interface (API) where three different existing simulation APIs for different scenarios can be called in a uniform way. A virtual photon or neutron facility experiment consists of a sequence of simulations describing the physical and conceptual entities of the experiment. In the framework of VINYL, the simulation starts from the source followed by the propagation of the beam through the beamline optics, then considers the complex process of the interaction of the beam with the sample, such as radiation damage, and eventually ends at the simulation of the scattered intensities. Various simulation modules are implemented for different simulation stages. For example, in order to gain an atomistic understanding of the photon-matter interaction, elementary quantum mechanical processes, associated changes in the structural, electronic, photophysical response of the excited system, Atomistic Simulations Environment (ASE)[3] has been utilized for the sample trajectory simulation.

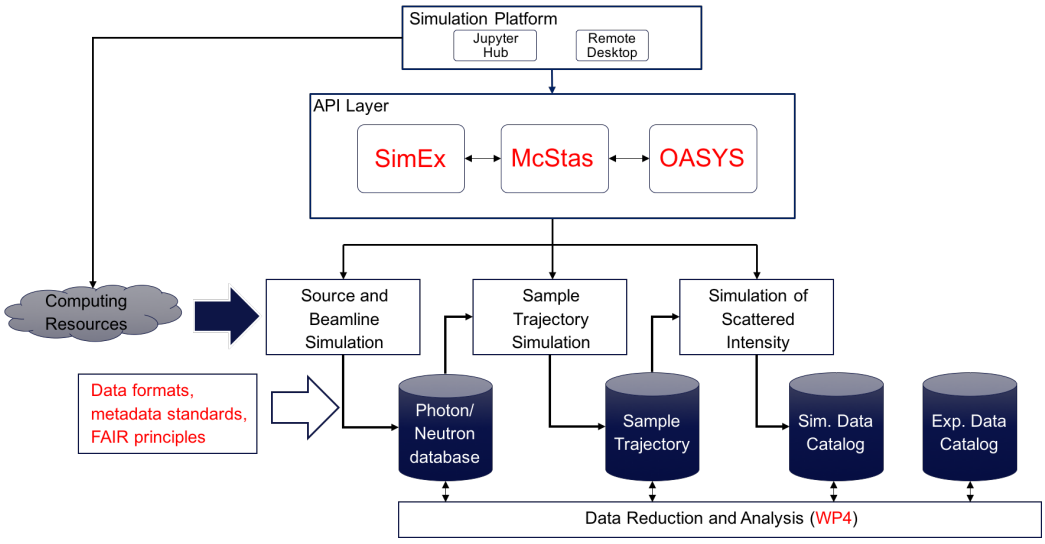

Figure 1. The schematic of the elements of the VINYL virtual facility.

2.1 Interfacing data format Standards drafted for VINYL

There are various simulation codes involved in the simulation pipeline. These codes are developed in different groups with different input/output data format definitions. In order to achieve seamless exchange of data between simulation software in simulation pipelines, a standardized formatting and hierarchical organization of simulation

data is needed. At the same time, this kind of format standard can also benefit from 3rd party data visualization and analysis software that support these formats.

We choose openPMD[4] meta data standard as the interfacing data format, therefore our workflows and results become accessible, inter–operable, and reusable to stay in line with the core concepts of FAIR Data Principles.[5] OpenPMD stands for open particle and mesh data. It was initially developed as a metadata and data hierarchy standard for particle–in–cell (PIC) simulations of high–power laser–matter interaction at the Helmholtz–Zentrum Dresden–Rossendorf. It is currently not only limited to define PIC simulation data, but, thanks to its flexibility, also widely adopted in numerous simulation codes, visualization codes, and simulation workflow platforms by defining the domain extension in addition to the base standard. The data conforming openPMD standard can be naturally written in hierarchical file formats, such as HDF5, ADIOS1, ADIOS2[6] and JSON. It is noteworthy that the streaming function provided by ADIOS2 is promising to speed up the computing in the workflow where a large amount of data needs to be passed from one program to another.

In VINYL, we have defined the domain extensions for coherent wavefront propagation, photon raytracing, neutron raytracing and molecular dynamics simulations to support the data exchange between the simulation modules. The extensions can be found here: https://github.com/PaNOSC-ViNYL/openPMD-standard/tree/upcoming-2.0.0.

2.2 Simulation backends

In VINYL, three existed simulation applications are considered as the backends of the API: SimEx, OASYS and McStas.

SimEx[7] is the API of the SIMEX platform for simulation of experiments at advanced laser and X-ray light sources. It brings all aspects of typical experiments at light source infrastructures into a streamline of simulation. The simulations of photon source, light transport through optics elements in the beamline, interaction with a target or sample, scattering from the latter, photon detection, and data analysis can be done with various modules within the framework. The simulation framework has been actively used for single particle imaging studies.[8,9]

OASYS (OrAnge SYnchrotron Suite) is a versatile and user-friendly container of APIs dedicated to optical simulations.[10] It can provide a graphical environment for modelling X-ray experiments. Shadow, SRW, XOPPY, Syned are now available in OASYS. A new wave optics-based simulation package, WISEr, which is targeted at the simulation of the focusing performance of grazing X-ray optics systems, is now under developing and is fully integrable with OASYS. By implementing the photon raytracing interfacing data format, SimEx can obtain propagated beam parameters from the raytraycing simulation results of OASYS and then conduct the photon-mater interaction simulations making use of the beam parameters.

McStas[11,12] is a general software package for Monte Carlo neutron ray-tracing simulations. The developing of it started about 20 years ago and is still on going. McStats consists of a number of components files to describe the corresponding beam-optical components in real experiments. The experimental instrument is represented by an instrumental file containing a selection of components and their position and orientation. In order to make use of today's cloud computing service technology and to harmonize the usage of McStas to be compatible with VINYL, a python API, McStasScript[13] was developed. McStasScript allows a user to create instrument models and handle the returned data including plotting. Existing McStas projects can be converted to python using tools included in the McStasScript package.

3. APPLICATION CASES

During the development of the virtual laboratory, several simulation modules have been implemented in some typical scenarios to demonstrate their use for practical simulations.

```
beam_parameters = PhotonBeamParameters(
            photon_energy = 8.0e3*electronvolt,
            pulse_energy = 2.4e-6*joule,
            photon_energy_relative_bandwidth=1e-4,
            divergence=2.0e-6*radian,
            photon_energy_spectrum_type=None,
            beam_diameter_fwhm = None
            )
```

Figure 2. The parameters of a Gaussian source resemble to an ideal hard X-ray source defined in a jupyter notebook cell.

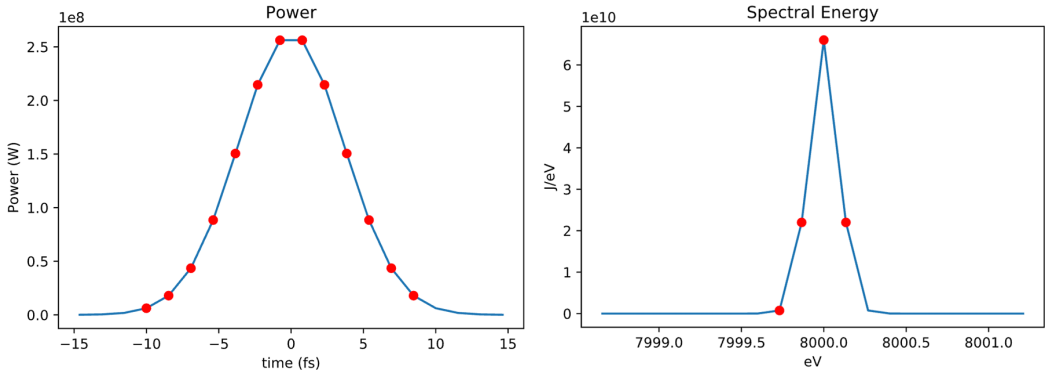

Figure 3. The temporal and spectral profiles of the Gaussian X-ray source plotted by the analysis functions of SimEx.

3.1 X-ray Gaussian source and its propagation

This example is a quickstart example for users to get familiar with the usage of the SimEx API. An X-ray source with Gaussian distribution, both temporal and spatial, is the simplest description for starting a wavefront propagation simulation.

The source is defined by its photon energy, pulse energy and photon energy relative bandwidth as shown in Fig. 2 in one jupyter notebook cell. SimEx also provides analysis functions to visualize the temporal and spectral profiles (Fig. 3) and wavefront intensity map of a 2D slice (Fig. 4). After saving the source file in HDF5 format, the output can then be input into wave propagation modules, such as WPG[14] to continue the start-to-end simulation by, for eaxmple, simulating the propagation and focusing of the X-ray beam for specific X-ray optics and geometries.

3.2 Serial crystallography diffraction at European XFEL

Serial femtosecond crystallography (SFX) is a method to determine atomic-scale structures from many individual crystals of a given sample. One prevalent problem in conventional macromolecular X-ray crystallography is the difficulty in forming high diffraction quality crystals.[15] Besides that, the strong radiation damage has hindered the structure determination of nanocrystals. Making use of the extra-high brilliance and ultra-short pulse (tens of femtoseconds) of XFELs, SFX makes it possible to measure the structures of micrometer-sized and smaller protein crystals at room temperature and to potentially study biomolecular dynamics using time-resolved experimental measurements.[16,17] The megahertz pulse repetition rate achieved at the European XFEL[18] can provide efficient measurements of the data volumes necessary for high resolution time-resolved studies in a relatively short time. By collecting a large dataset of diffraction patterns from nano/micrometer sized crystals, which are delivered by liquid jets, a number of experimental results[19–24] have shown the prospects of this method and make it a class of experiments where simulation may also help provide insight and direction.

The 1 megapixel Adaptive Gain Integrating Pixel Detector (AGIPD)[25] is the most commonly used diffraction detector in the SPB/SFX instrument of the European XFEL. As shown in the schematic in Fig. 5 generated by EXtra-geom,[26] this 1M AGIPD detector consists of 4 movable quadrants, each having 4 detector tiles with

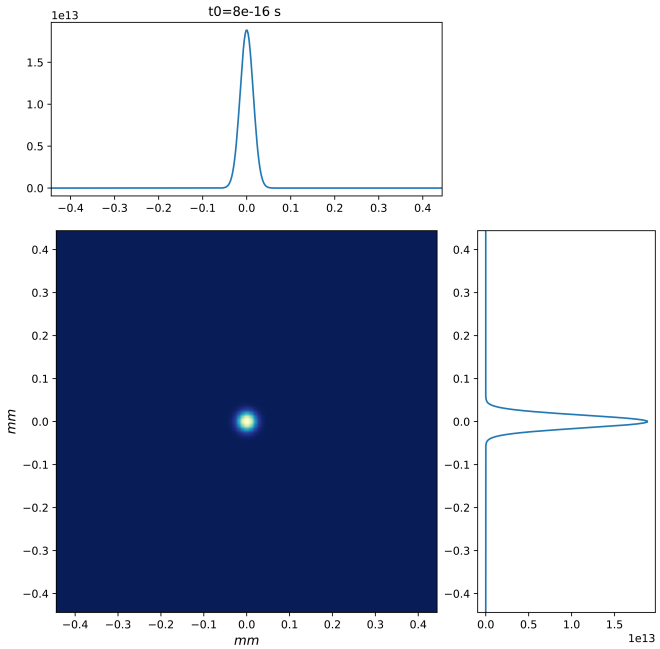

Figure 4. The intensity map of a 2D slice from the Gaussian X-ray source plotted by the analysis functions of SimEx.

512 × 128 pixels per tile. Each tile is further divided into 2 × 8 individual Application Specific Integrated Circuits (ASICs), each having 64 × 64 pixels of size 200 μm × 200 μm. Since the ASICs cannot physically touch each other, a gap covering the area of two ordinary pixels exists horizontally.

ADU noise, non-functional pixels and diffraction from the medium in which crystals are suspended will all add complications to extracting the exact structure information from diffraction patterns. In this example, ideal noise-free monolithic diffraction patterns and diffraction patterns on multiple detector panels are simulated using SimEx respectively and analysed with CrystFEL[27] to show the effects of the gaps between detector panels on the results of crystallography analysis.

We generate 200 diffraction patterns of perfect lysozyme crystals (PDB structure 3WUL[22]) for both groups (monolithic and multiple-panel detector) using the CrystFEL diffraction calculator in SimEx. The X-ray beam is ideally monochromatic with photon energy of 4.972 keV and focus diameter of 130 nm. The sample-to-detector distance is 130 mm. For the noise-free monolithic diffraction patterns (Fig. 6 (a)), we use a setup of 1000 × 1000 pixels of 220 × 220 μm^2 size to make it comparable to the multiple-panel diffraction patterns (Fig. 6 (b)) generated with AGIPD geometry. Random rotation of the crystal is implemented during simulation to imitate the the random orientation of the sample in the experiment.

The diffraction patterns are then indexed with CrystFEL's indexamajig tool, to estimate the unit cell parameters - the three lengths and three angles which describe the repeating unit of the crystal structure. In Fig. 7, the unit cell estimates from the monolithic diffraction patterns are tightly clustered around the expected values for lysozyme. By comparison, the estimates in Fig. 8 from the multi-panel diffraction patterns show markedly different distributions: there are still clear peaks at the expected values, but there is a much wider spread of bad estimates for each parameter. This test case didn't explore different analysis parameters which may have refined or filtered out these results.

This example demonstrates the functionality of SimEx to consider the multi-panel detector geometry. The analysis results indicate that the gaps between detector panels may yield errors in the estimation of cell parameters. This may result from the information missed in the gap. Noticing that only 200 patterns are included in the dataset, one notes that a larger dataset may help reduce the errors.

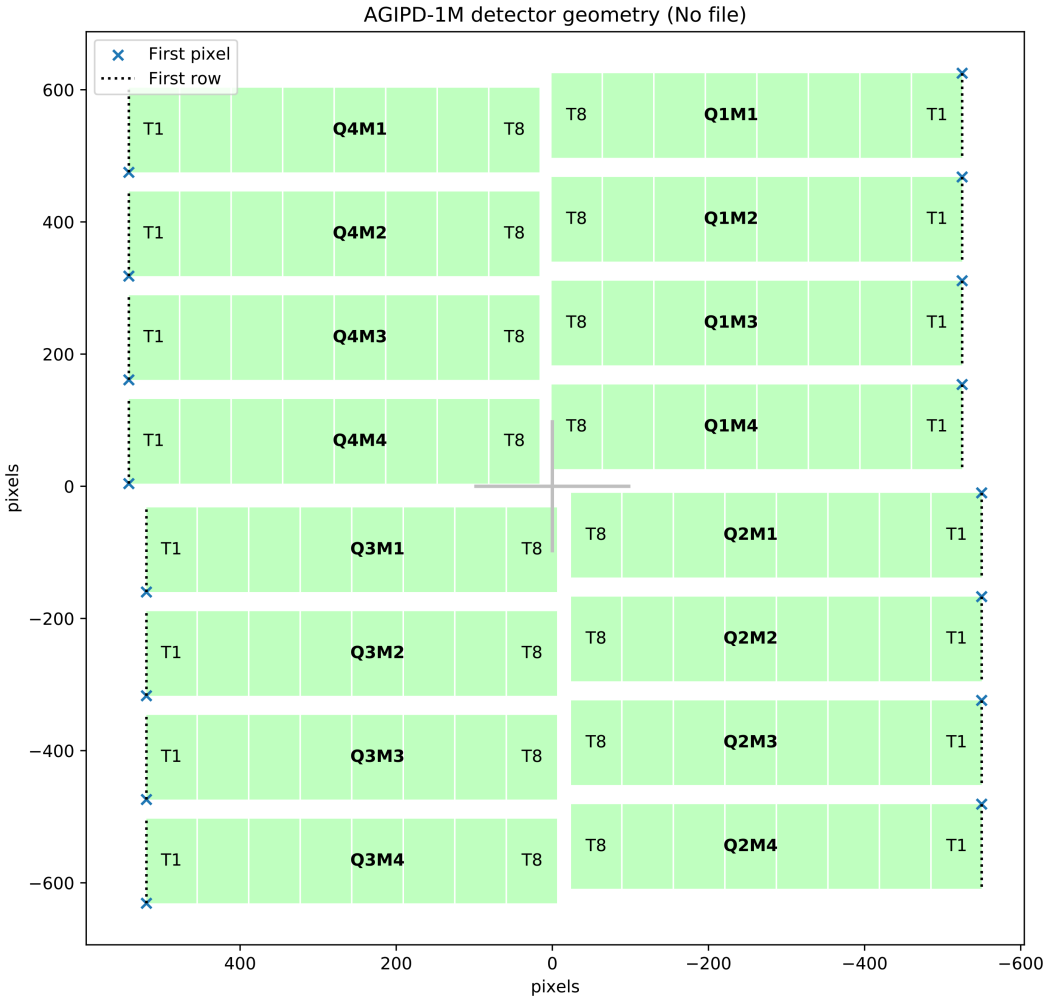

Figure 5. The detector geometry of AGIPD.

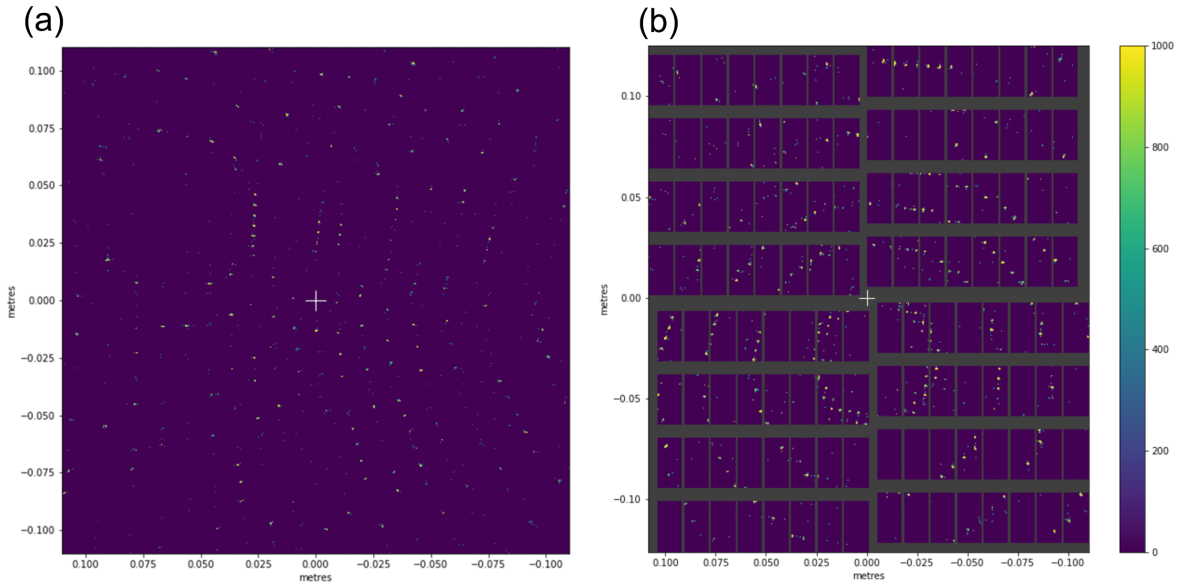

Figure 6. The snapshots of generated datasets of (a) monolithic diffraction patters and (b) multiple-panel diffraction patterns. Since random rotation is implemented during simulation, the two diffraction patterns look different.

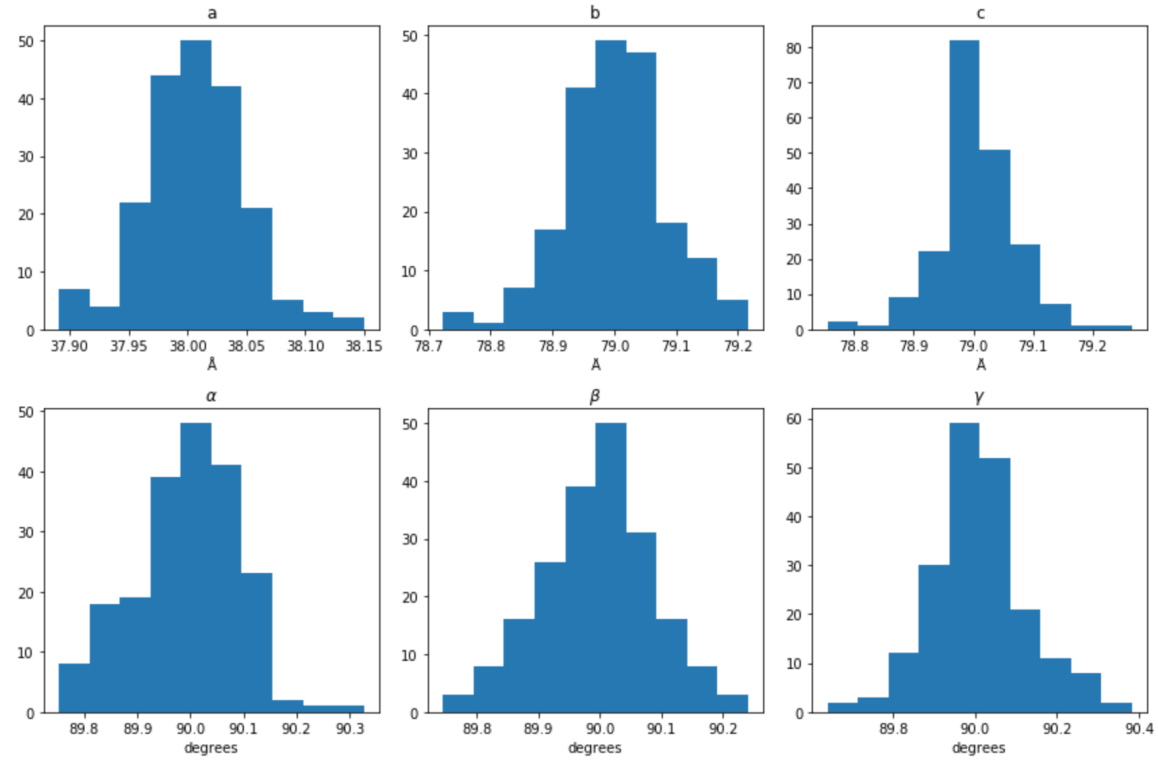

Figure 7. The statistics of the cell parameters estimated from the monolithic diffraction patterns: a, b and c are the length of each side of the unit cell and α, β and γ are the angles between these sides. The y-axis is the frequency of each value of the lattice parameters on the x-axis.

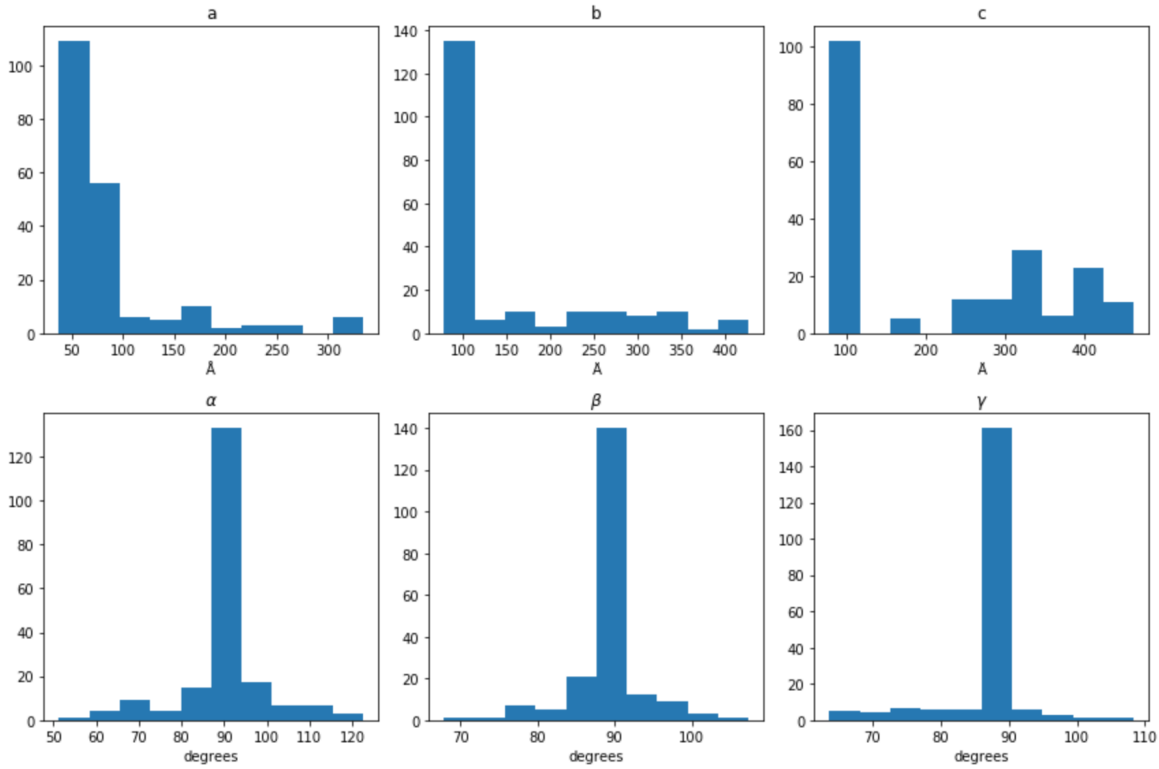

Figure 8. The statistics of the cell parameters estimated from the multi-panel diffraction patterns: a, b and c are the length of each side of the unit cell and α, β and γ are the angles between these sides. The y-axis is the frequency of each value of the lattice parameters on the x-axis.

3.3 Polychromatic diffraction simulation using OASYS and SimEx

As an exercise to bring the SimEx photon simulation framework and OASYS optical simulation environment together, several demo jupyter notebooks are created to show how SimEx takes the output data of OASYS complying with the openPMD wavefront domain extension defined in https://github.com/PaNOSC-ViNYL/openPMD-standard/blob/upcoming-2.0.0/EXT_PRAYTRACE.md and generates the diffraction patterns using the GAPD[28] diffraction calculator integrated in SimEx with the wavefront data.

In this application case, we simulate the X-ray wavefront using OASYS. Beamline ID23 at ESRF[29] has been used as an example. It consists of a slit, Si-111 monochromator (E = 14.2 keV) and a KB-focusing mirror system. A ray-tracing simulation using ShadowOui package has been performed. For demonstration purposes a low number of rays (10^6) and a narrow energy bandwitdh has been used. The workflow has been demonstrated in two ways. The first is using OASYS capability to generate the underlying Python code for running the simulation made in the GUI and then running the said code in the Jupyter notebook of SimEx. The second way is to use OASYS capability to run native Python code in a GUI widget, where the beamline output is linked directly to a series of two widgets: one exporting the wavefront to openPMD output and the other one containing SimEx code. The wavefront output, as shown in Fig. 9 (a), is generated in the format conforming the openPMD Domain-Specific Naming Conventions for Photon Raytracing Codes and then used as a input in the diffraction simulation within the SimEx framework. The diffraction simulation is conducted on a single crystal Cu sample using the GAPD diffraction calculator, the result is presented in Fig. 9 (b).

This example has demonstrated how different backends in VINYL work together to complete the start-to-end simulation workflow.

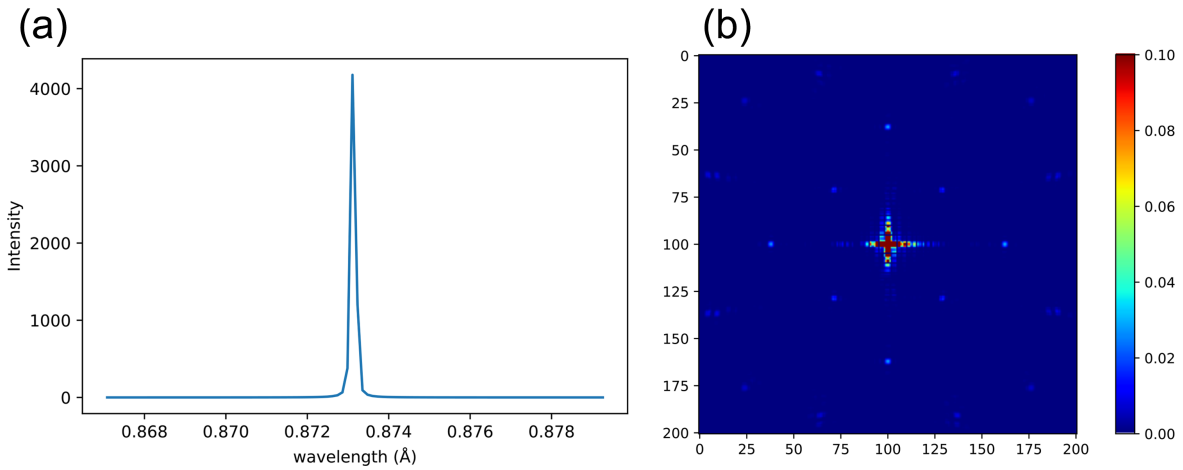

Figure 9. (a) The X-ray spectrum obtained from OASYS. (b) The diffraction pattern simulated with the X-ray spectrum in (a) and single crystal Cu sample using the GAPD calculator of SimEx.

4. CONCLUSIONS

VINYL will be a simulation platform providing a harmonized API to conduct a simulation from the source to the detector representing the major components of photon and neutron RIs. These types of simulation will ultimately help design and optimize experiment setups, estimate experiment artifacts, generate supporting material for beamtime proposals, assist in decision making during an ongoing experiment (for example, when to adjust experiment parameters), and ultimately contribute to the interpretation of experimental results.

ACKNOWLEDGMENTS

This work is funded by the European Union's Horizon 2020 research and innovation programme under grant agreement No. 823852.

REFERENCES

[1] "The Photon and Neutron Open Science Cloud (PaNOSC)." https://www.panosc.eu/.

[2] Kluyver, T., Ragan-Kelley, B., Pérez, F., Granger, B. E., Bussonnier, M., Frederic, J., Kelley, K., Hamrick, J. B., Grout, J., and Corlay, S., "Jupyter Notebooks-a publishing format for reproducible computational workflows.," in [*ELPUB*], 87–90 (2016).

[3] Larsen, A. H., Mortensen, J. J., Blomqvist, J., Castelli, I. E., Christensen, R., Du\lak, M., Friis, J., Groves, M. N., Hammer, B., Hargus, C., Hermes, E. D., Jennings, P. C., Jensen, P. B., Kermode, J., Kitchin, J. R., Kolsbjerg, E. L., Kubal, J., Kaasbjerg, K., Lysgaard, S., Maronsson, J. B., Maxson, T., Olsen, T., Pastewka, L., Peterson, A., Rostgaard, C., Schiøtz, J., Schütt, O., Strange, M., Thygesen, K. S., Vegge, T., Vilhelmsen, L., Walter, M., Zeng, Z., and Jacobsen, K. W., "The atomic simulation environment—a Python library for working with atoms," *Journal of Physics: Condensed Matter* **29**, 273002 (June 2017).

[4] Huebl, A., Lehe, R., Vay, J.-L., Grote, D. P., Sbalzarini, I., Kuschel, S., and Bussmann, M., "Openpmd 1.0.0: A meta data standard for particle and mesh based data." https://dx.doi.org/10.5281/zenodo.33624 (2017).

[5] Wilkinson, M. D., Dumontier, M., Aalbersberg, I. J., Appleton, G., Axton, M., Baak, A., Blomberg, N., Boiten, J.-W., da Silva Santos, L. B., Bourne, P. E., Bouwman, J., Brookes, A. J., Clark, T., Crosas, M., Dillo, I., Dumon, O., Edmunds, S., Evelo, C. T., Finkers, R., Gonzalez-Beltran, A., Gray, A. J., Groth, P., Goble, C., Grethe, J. S., Heringa, J., Hoen, P. A. ´., Hooft, R., Kuhn, T., Kok, R., Kok, J., Lusher, S. J., Martone, M. E., Mons, A., Packer, A. L., Persson, B., Rocca-Serra, P., Roos, M., van Schaik, R., Sansone, S.-A., Schultes, E., Sengstag, T., Slater, T., Strawn, G., Swertz, M. A., Thompson, M., van der Lei, J., van Mulligen, E., Velterop, J., Waagmeester, A., Wittenburg, P., Wolstencroft, K., Zhao, J., and Mons, B.,

"The FAIR guiding principles for scientific data management and stewardship," *Scientific Data* **3**, 160018 (mar 2016).

[6] Godoy, W. F., Podhorszki, N., Wang, R., Atkins, C., Eisenhauer, G., Gu, J., Davis, P., Choi, J., Germaschewski, K., Huck, K., Huebl, A., Kim, M., Kress, J., Kurc, T., Liu, Q., Logan, J., Mehta, K., Ostrouchov, G., Parashar, M., Poeschel, F., Pugmire, D., Suchyta, E., Takahashi, K., Thompson, N., Tsutsumi, S., Wan, L., Wolf, M., Wu, K., and Klasky, S., "ADIOS 2: The Adaptable Input Output System. A framework for high-performance data management," *SoftwareX* **12**, 100561 (July 2020).

[7] "PaNOSC-ViNYL/SimEx." https://github.com/PaNOSC-ViNYL/SimEx (May 2020).

[8] Yoon, C. H., Yurkov, M. V., Schneidmiller, E. A., Samoylova, L., Buzmakov, A., Jurek, Z., Ziaja, B., Santra, R., Loh, N. D., Tschentscher, T., and Mancuso, A. P., "A comprehensive simulation framework for imaging single particles and biomolecules at the European X-ray Free-Electron Laser," *Scientific Reports* **6** (Apr. 2016).

[9] Fortmann-Grote, C., Buzmakov, A., Jurek, Z., Loh, N.-T. D., Samoylova, L., Santra, R., Schneidmiller, E. A., Tschentscher, T., Yakubov, S., Yoon, C. H., Yurkov, M. V., Ziaja-Motyka, B., and Mancuso, A. P., "Start-to-end simulation of single-particle imaging using ultra-short pulses at the European X-ray Free-Electron Laser," *IUCrJ* **4**, 560–568 (Sept. 2017).

[10] Rebuffi, L. and Sanchez del Rio, M., "OASYS (OrAnge SYnchrotron Suite): An open-source graphical environment for x-ray virtual experiments," in [*Advances in Computational Methods for X-Ray Optics IV*], Sawhney, K. and Chubar, O., eds., 28, SPIE, San Diego, United States (Aug. 2017).

[11] Lefmann, K. and Nielsen, K., "McStas, a general software package for neutron ray-tracing simulations," *Neutron News* **10**, 20–23 (Jan. 1999).

[12] Willendrup, P. K. and Lefmann, K., "McStas: Introduction, use, and basic principles for ray-tracing simulations," *Journal of Neutron Research* **22**, 1–16 (Apr. 2020).

[13] "PaNOSC-ViNYL/McStasScript." https://github.com/PaNOSC-ViNYL/McStasScript (May 2020).

[14] Samoylova, L., Buzmakov, A., Chubar, O., and Sinn, H., "*WavePropaGator* : Interactive framework for X-ray free-electron laser optics design and simulations," *Journal of Applied Crystallography* **49**, 1347–1355 (Aug. 2016).

[15] Martin-Garcia, J. M., Conrad, C. E., Coe, J., Roy-Chowdhury, S., and Fromme, P., "Serial femtosecond crystallography: A revolution in structural biology," *Archives of Biochemistry and Biophysics* **602**, 32–47 (July 2016).

[16] Tenboer, J., Basu, S., Zatsepin, N., Pande, K., Milathianaki, D., Frank, M., Hunter, M., Boutet, S., Williams, G. J., Koglin, J. E., Oberthuer, D., Heymann, M., Kupitz, C., Conrad, C., Coe, J., Roy-Chowdhury, S., Weierstall, U., James, D., Wang, D., Grant, T., Barty, A., Yefanov, O., Scales, J., Gati, C., Seuring, C., Srajer, V., Henning, R., Schwander, P., Fromme, R., Ourmazd, A., Moffat, K., Van Thor, J., Spence, J. H. C., Fromme, P., Chapman, H. N., and Schmidt, M., "Time-Resolved Serial Crystallography Captures High Resolution Intermediates of Photoactive Yellow Protein," *Science (New York, N.Y.)* **346**, 1242–1246 (Dec. 2014).

[17] Spence, J. C. H., "XFELs for structure and dynamics in biology," *IUCrJ* **4**, 322–339 (July 2017).

[18] Yefanov, O., Oberthür, D., Bean, R., Wiedorn, M. O., Knoska, J., Pena, G., Awel, S., Gumprecht, L., Domaracky, M., Sarrou, I., Lourdu Xavier, P., Metz, M., Bajt, S., Mariani, V., Gevorkov, Y., White, T. A., Tolstikova, A., Villanueva-Perez, P., Seuring, C., Aplin, S., Estillore, A. D., Küpper, J., Klyuev, A., Kuhn, M., Laurus, T., Graafsma, H., Monteiro, D. C. F., Trebbin, M., Maia, F. R. N. C., Cruz-Mazo, F., Gañán-Calvo, A. M., Heymann, M., Darmanin, C., Abbey, B., Schmidt, M., Fromme, P., Giewekemeyer, K., Sikorski, M., Graceffa, R., Vagovic, P., Kluyver, T., Bergemann, M., Fangohr, H., Sztuk-Dambietz, J., Hauf, S., Raab, N., Bondar, V., Mancuso, A. P., Chapman, H., and Barty, A., "Evaluation of serial crystallographic structure determination within megahertz pulse trains," *Structural Dynamics* **6**, 064702 (Nov. 2019).

[19] Chapman, H. N., Fromme, P., Barty, A., White, T. A., Kirian, R. A., Aquila, A., Hunter, M. S., Schulz, J., DePonte, D. P., and Weierstall, U., "Femtosecond X-ray protein nanocrystallography," *Nature* **470**(7332), 73–77 (2011).

[20] Aquila, A., Hunter, M. S., Doak, R. B., Kirian, R. A., Fromme, P., White, T. A., Andreasson, J., Arnlund, D., Bajt, S., and Barends, T. R., "Time-resolved protein nanocrystallography using an X-ray free-electron laser," *Optics express* **20**(3), 2706–2716 (2012).

[21] Barty, A., Caleman, C., Aquila, A., Timneanu, N., Lomb, L., White, T. A., Andreasson, J., Arnlund, D., Bajt, S., and Barends, T. R., "Self-terminating diffraction gates femtosecond X-ray nanocrystallography measurements," *Nature photonics* **6**(1), 35–40 (2012).

[22] Sugahara, M., Mizohata, E., Nango, E., Suzuki, M., Tanaka, T., Masuda, T., Tanaka, R., Shimamura, T., Tanaka, Y., and Suno, C., "Grease matrix as a versatile carrier of proteins for serial crystallography," *Nature methods* **12**(1), 61–63 (2015).

[23] Wiedorn, M. O., Oberthür, D., Bean, R., Schubert, R., Werner, N., Abbey, B., Aepfelbacher, M., Adriano, L., Allahgholi, A., Al-Qudami, N., Andreasson, J., Aplin, S., Awel, S., Ayyer, K., Bajt, S., Barák, I., Bari, S., Bielecki, J., Botha, S., Boukhelef, D., Brehm, W., Brockhauser, S., Cheviakov, I., Coleman, M. A., Cruz-Mazo, F., Danilevski, C., Darmanin, C., Doak, R. B., Domaracky, M., Dörner, K., Du, Y., Fangohr, H., Fleckenstein, H., Frank, M., Fromme, P., Gañán-Calvo, A. M., Gevorkov, Y., Giewekemeyer, K., Ginn, H. M., Graafsma, H., Graceffa, R., Greiffenberg, D., Gumprecht, L., Göttlicher, P., Hajdu, J., Hauf, S., Heymann, M., Holmes, S., Horke, D. A., Hunter, M. S., Imlau, S., Kaukher, A., Kim, Y., Klyuev, A., Knoška, J., Kobe, B., Kuhn, M., Kupitz, C., Küpper, J., Lahey-Rudolph, J. M., Laurus, T., Le Cong, K., Letrun, R., Xavier, P. L., Maia, L., Maia, F. R. N. C., Mariani, V., Messerschmidt, M., Metz, M., Mezza, D., Michelat, T., Mills, G., Monteiro, D. C. F., Morgan, A., Mühlig, K., Munke, A., Münnich, A., Nette, J., Nugent, K. A., Nuguid, T., Orville, A. M., Pandey, S., Pena, G., Villanueva-Perez, P., Poehlsen, J., Previtali, G., Redecke, L., Riekehr, W. M., Rohde, H., Round, A., Safenreiter, T., Sarrou, I., Sato, T., Schmidt, M., Schmitt, B., Schönherr, R., Schulz, J., Sellberg, J. A., Seibert, M. M., Seuring, C., Shelby, M. L., Shoeman, R. L., Sikorski, M., Silenzi, A., Stan, C. A., Shi, X., Stern, S., Sztuk-Dambietz, J., Szuba, J., Tolstikova, A., Trebbin, M., Trunk, U., Vagovic, P., Ve, T., Weinhausen, B., White, T. A., Wrona, K., Xu, C., Yefanov, O., Zatsepin, N., Zhang, J., Perbandt, M., Mancuso, A. P., Betzel, C., Chapman, H., and Barty, A., "Megahertz serial crystallography," *Nature Communications* **9** (Dec. 2018).

[24] Pandey, S., Bean, R., Sato, T., Poudyal, I., Bielecki, J., Cruz Villarreal, J., Yefanov, O., Mariani, V., White, T. A., Kupitz, C., Hunter, M., Abdellatif, M. H., Bajt, S., Bondar, V., Echelmeier, A., Doppler, D., Emons, M., Frank, M., Fromme, R., Gevorkov, Y., Giovanetti, G., Jiang, M., Kim, D., Kim, Y., Kirkwood, H., Klimovskaia, A., Knoska, J., Koua, F. H. M., Letrun, R., Lisova, S., Maia, L., Mazalova, V., Meza, D., Michelat, T., Ourmazd, A., Palmer, G., Ramilli, M., Schubert, R., Schwander, P., Silenzi, A., Sztuk-Dambietz, J., Tolstikova, A., Chapman, H. N., Ros, A., Barty, A., Fromme, P., Mancuso, A. P., and Schmidt, M., "Time-resolved serial femtosecond crystallography at the European XFEL," *Nature Methods* **17**, 73–78 (Jan. 2020).

[25] Allahgholi, A., Becker, J., Delfs, A., Dinapoli, R., Goettlicher, P., Greiffenberg, D., Henrich, B., Hirsemann, H., Kuhn, M., Klanner, R., Klyuev, A., Krueger, H., Lange, S., Laurus, T., Marras, A., Mezza, D., Mozzanica, A., Niemann, M., Poehlsen, J., Schwandt, J., Sheviakov, I., Shi, X., Smoljanin, S., Steffen, L., Sztuk-Dambietz, J., Trunk, U., Xia, Q., Zeribi, M., Zhang, J., Zimmer, M., Schmitt, B., and Graafsma, H., "The Adaptive Gain Integrating Pixel Detector at the European XFEL," *Journal of Synchrotron Radiation* **26**, 74–82 (Jan. 2019).

[26] "EXtra-geom: X-ray detector geometry for European XFEL — EXtra-geom 0.10.0 documentation." https://extra-geom.readthedocs.io/en/latest/index.html.

[27] White, T. A., Kirian, R. A., Martin, A. V., Aquila, A., Nass, K., Barty, A., and Chapman, H. N., "*CrystFEL* : A software suite for snapshot serial crystallography," *Journal of Applied Crystallography* **45**, 335–341 (Apr. 2012).

[28] E, J. C., Wang, L., Chen, S., Zhang, Y. Y., and Luo, S. N., "*GAPD* : A GPU-accelerated atom-based polychromatic diffraction simulation code," *Journal of Synchrotron Radiation* **25**, 604–611 (Mar. 2018).

[29] Flot, D., Mairs, T., Giraud, T., Guijarro, M., Lesourd, M., Rey, V., Van Brussel, D., Morawe, C., Borel, C., and Hignette, O., "The ID23-2 structural biology microfocus beamline at the ESRF," *Journal of Synchrotron Radiation* **17**(1), 107–118 (2010).